2E1-2

Deection of Bubble Size and Location using Ultrasound Simulation with Machine Learning

Zi Wang[1†], Shu Takagi[1*], and Yoshiki Watanabe[1]
([1] Grad. School Eng., The Univ. of Tokyo)

1. Background & Objective

The deep ocean, a vast and largely unexplored frontier, harbors immense economic and scientific potential. In the realm of deep-sea mining, air-lift pumps [1)] (see Figure 1) have emerged as a promising method for extracting Rare-Earth Elements (REE) [2)]. Despite proposals for their use, the current technology remains immature. Takagi et al. [3)] conducted experiments and numerical simulations to investigate multiphase flow mechanisms within air-lift pump systems. Sequential monitoring of flow patterns, essential for understanding airlift pumps, is yet to be developed. This study addresses these challenges using ultrasound imaging and machine learning [4)].

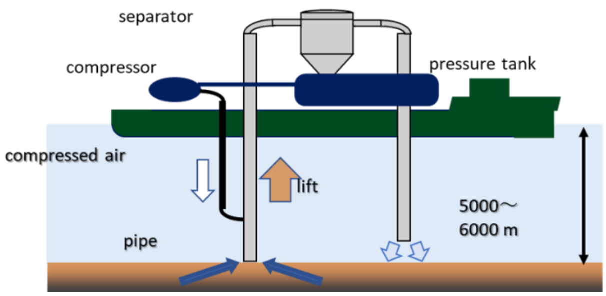

Figure 1: Structure of airlift pumps.

2. Simulation & Verification

To achieve high accuracy and enable direct processing of simulation results, we employ Direct Numerical Simulations (DNS). Utilizing the K-Wave package in MATLAB, we conduct simulations (see Figure 2), demonstrating the interpretation of Radio Frequency (RF) data (see Figure 3) and illustrating their graphical representation. Result verification is conducted to ensure the validity of acquired data. The Helmholtz equation is solved to further validate our simulation.

$$\nabla^2 p - \frac{1}{c_0^2}\frac{\partial^2 p}{\partial t^2} = 0 \ .$$

Importantly, the concept of subtraction is introduced to enhance location and size prediction, a key aspect for understanding bubble dynamics.

E-mail: †wanggs2021@g.ecc.u-tokyo.ac.jp,
*takagi@mech.t.u-tokyo.ac.jp

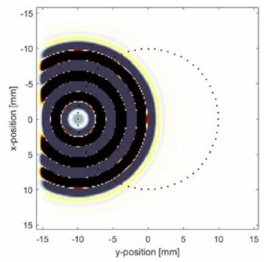

Figure 2: Example of ultrasound propagation.

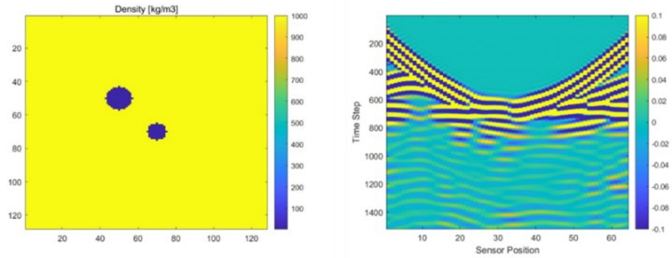

Figure 3: Example of simulation results of RF data.

3. Full Waveform Inversion

Full Waveform Inversion is a well known solution for inverse problems. We conducted calculation of FWI and have found that FWI is not reliable as transducer numbers decrease. Artifacts occur frequently. Small particles are hard to be distinguished especially when complexed surroundings. (see Figure 4)

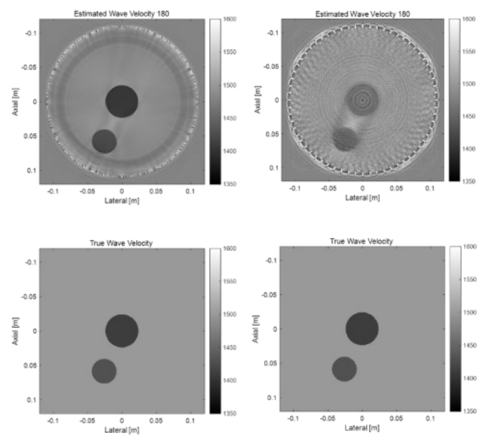

Figure 4: FWI reproduction for 512 and 64 transducers

4. Machine Learning Techniques

Machine learning techniques play a crucial role in our research. The project evaluates different machine learning algorithms, highlighting their pros and cons. The impact of datasets and data types on training performance is also discussed. We propose a balanced combination of a large dataset and representative data augmentation techniques to enhance model accuracy and robustness. The machine learning settings and algorithm structure are clearly presented through figures and tables. Training results, along with reasons for suboptimal accuracy and drawbacks of computer knowledge-based algorithms, are illustrated and analyzed. Despite achieving 70% accuracy using skip connect [5] and CNN, these methods lack physics-informed elements, falling short of our expectations.

5. Postprocessing and natural image dataset

Introducing a new postprocessing skill using subtraction (See Figure 5), we combine it with machine learning training results. Before formal application, the sensitivity of the subtraction method is tested and confirmed applicable for most cases. We propose a complete and novel technique for postprocessing training results. This section introduces additional transducers for postprocessing-assisted deep learning, surpassing the limitations discussed earlier. Based on our innovative methods and different transducer numbers, the results demonstrate increased accuracy, particularly with 8 transducers, achieving above 80% accuracy. For 2&3 bubbles problem, an average accuracy of 95% is attained. (See Table 1)

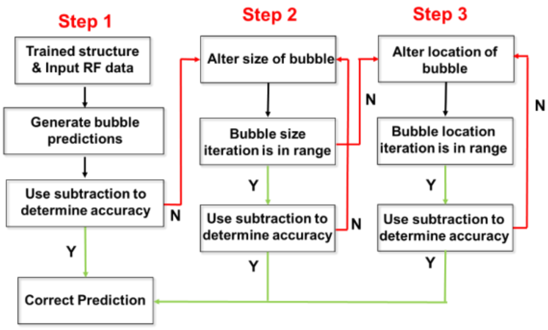

Figure 5: Structure of postprocessing.

Bubble numbers	Location accuracy	Modified location accuracy	Size accuracy	Modified size accuracy
2 bubbles	96.3%	99.9%(+3.6)	87.0%	99.9%(+12.9)
3 bubbles	90.8%	96.1%(+5.3)	77.0%	95.7%(+18.7)
4 bubbles	88.7%	92.7%(+4.0)	81.6%	89.4%(+7.8)
5 bubbles	78.1%	86.2%(+8.1)	74.3%	80.3%(+7.0)

Table 1: Accuracy comparison of predictions.

Natural image dataset could also be used for machine learning training. [6] According to our training result, natural image dataset and the structure shows good generalization ability. (See Figure 6 & Table 2)

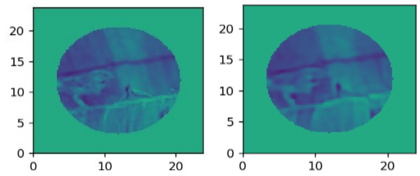

Figure 6: Result of Natural image set training.

Dataset types	SOS - MAE	Density - MAE
Distorted bubbles	5.68 ± 5.78	11.34 ± 9.22
Natural images	4.85 ± 5.08	8.47 ± 8.50

Table 2: Accuracy comparison of datasets.

6. Current & Future Works

Currently we are working on 3D situations of this ultrasound-based detection task. The feature of 3D spaces leads to the difficulty of building models of bubbles and lengthen the simulation time to tens of times of 2D cases. The setting of transducers is being tried under different pitch size and layout considering possible interactions under spatial conditions.

Our process is expected to complete the current task by the time of the conference so that we could include the contents for 3D cases. 3D cases are rarely considered, and it is worthy discussion for possible solutions. After current works, future works may include more experiments on real-world data, addressing irregular bubble shapes, investigating gas-liquid-solid 3-phase interactions.

References

1) Takaya. Y, et al., Scientific Reports., 8(2018), No.5763.
2) Saito. T, et.al., In: Proceedings OCEANS, (1989), No.592812.
3) Kazuya Shimizu, Shu Takagi, IJMF, Vol.142 (2021), 10-3726.
4) Haas, Tim, et al. Chem Eng. Science 216 (2020): 115467.
5) He. K, et al. *Deep residual learning for image recognition*, IEEE. 2016: 770-778.
6) Watanabe Y, et.al., Applied Sciences, 2023, 14(1): 37.